

Complex scattering lengths for ultracold He collisions with rotationally excited linear and nonlinear molecules

Benhui Yang,^{1,*} R. C. Forrey,² P. C. Stancil,¹ and N. Balakrishnan³

¹*Department of Physics and Astronomy and the Center for Simulational Physics, The University of Georgia, Athens, Georgia 30602, USA*

²*Department of Physics, Penn State University, Berks Campus, Reading, Pennsylvania 19610, USA*

³*Department of Chemistry, University of Nevada Las Vegas, Las Vegas, Nevada 89154, USA*

(Received 29 July 2010; published 30 November 2010)

The translational and internal level cooling of atoms and molecules in ultracold gases results from a combination of elastic and inelastic collisional processes. While elastic collisions lead to rapid thermalization, exoergic inelastic collisions may lead to heating and trap loss. To date, most collisional studies have targeted low-lying levels of diatomic molecules. Here we investigate inelastic quenching and elastic scattering of rotationally excited linear (H_2 , HD, CO, O_2 , and CO_2) and nonlinear (H_2O and NH_3) molecules in ultracold collisions with He and report the corresponding complex scattering lengths. It has been found that the ratio of the imaginary component β to the real component α of the scattering length generally increases with decreasing rotational constant for linear molecules. With the exception of CO, β becomes significantly smaller than α as the energy gap for rotational transitions increases. In all cases, β decreases with rotational energy gap for relatively large rotational excitation, allowing for convenient fits to an exponential energy gap formula. Excited rotational levels of H_2 and HD appear to be collisionally stable due to the very low values of β/α . Rotationally excited H_2O also appears to be a viable candidate for He buffer gas cooling due to relatively small values of β .

DOI: [10.1103/PhysRevA.82.052711](https://doi.org/10.1103/PhysRevA.82.052711)

PACS number(s): 34.50.Cx, 34.50.Ez

I. INTRODUCTION

Recent advances in cooling and trapping of molecules [1–3] have generated considerable interest in understanding atomic and molecular collisions at temperatures close to absolute zero. Theoretical studies of ultracold molecular collisions have largely centered around the vibrational and rotational relaxation of diatomic molecules induced by collisions with rare-gas atoms [2–5]. In these studies, it is generally found that the limiting values of the relaxation rate coefficients are strongly sensitive to the initial rovibrational levels of the molecules. The relaxation efficiency typically increases with vibrational level v and decreases with rotational level j , although there are deviations from these trends. In the widely used He buffer-gas cooling technique [6,7], thermalization of the rotational levels of the molecules usually occurs very rapidly so that nearly all of the cold molecules are in their rotational ground state. Therefore, a detailed understanding of rotational relaxation for these molecules is not required. With continued rapid advancements in the field of ultracold molecular physics, this situation may change. For example, an optical centrifuge [8] could be applied to a cold or ultracold gas to study cold collisions involving rotationally hot molecules. Other experimental schemes to produce translationally cold but rotationally hot molecules have also been proposed [9].

Theoretical studies have suggested that the collisional dynamics of rotationally hot molecules would be particularly interesting at low translational temperatures [10–17]. Rovibrational transitions that are quasis resonant (QR) at ordinary temperatures may become energetically inaccessible at cold or ultracold temperatures. When this happens, the dominant

pathway for relaxation is through pure rotational deexcitation. However, this relaxation pathway usually becomes increasingly less efficient as the rotational level is increased due to the widening internal energy gap between the initial and the final states of the molecule. Pure rotational deexcitation rate coefficients in the limit of zero temperature were shown to follow a smooth exponential energy gap dependence for He and Ar colliders with H_2 [13]. When this smooth exponentially decreasing behavior is included together with rovibrational transitions, sharp structures are seen in the rotational distributions of the total quenching rate coefficients at the boundaries where the quasis resonant vibration-rotation (QRVR) transfer channels are closed. Therefore, certain specific rotational levels may be considerably more stable against collisional relaxation than their neighboring rotational levels. The extent of this stability depends primarily on the efficiency of pure rotational quenching transitions.

In this work, we consider pure rotational relaxation at ultracold temperatures for a variety of collision systems in an effort to elucidate trends that may be explored in future ultracold molecule experiments. Quantum close-coupling (CC) and coupled-states (CS) scattering calculations are performed and the results are presented in terms of the real and imaginary parts of the complex scattering length. The survey includes linear molecules (H_2 , HD, CO, O_2 , and CO_2) and nonlinear molecules (H_2O and NH_3). Due to the importance of He in buffer-gas loading [6,7], sympathetic cooling [18], and helium cluster isolation spectroscopy [19], we selected He as the collision partner in each case. The diversity of molecules included in the survey should be useful for determining whether the exponential energy gap behavior seen in H_2 is a general feature of ultracold collisions. It also provides data that should be helpful for gaining a better understanding of the scale of the exponential energy gap behavior.

*yang@physast.uga.edu

II. THEORY

The s -wave scattering length plays an important role in the description of collisions at ultracold temperatures [20]. For internally excited molecules, it is convenient to describe the scattering properties in terms of a complex scattering length, $a = \alpha - i\beta$, where α and β are the real and imaginary components. The magnitude and sign of the real part α depend on the position of the last bound or virtual state of the collision complex relative to the dissociation limit. The imaginary part β is related to the total inelastic quenching cross section σ^{in} in the limit of zero velocity,

$$\beta = p\sigma^{\text{in}}/4\pi, \quad (1)$$

where p is the incident-channel wave vector. As $p \rightarrow 0$, the elastic scattering cross section is given by

$$\sigma^{\text{el}} = 4\pi(\alpha^2 + \beta^2). \quad (2)$$

While it is always possible to determine α from the limiting s -wave phase shift, it is often convenient to use Eqs. (1) and (2) to determine the magnitude of α :¹

$$|\alpha| = \sqrt{\sigma^{\text{el}}/4\pi - \beta^2}. \quad (3)$$

The elastic and inelastic cross sections, and consequently the components of the complex scattering length, are generally very sensitive to the details of the potential energy surface (PES). The ratio β/α is much less dependent on the properties of the PES and it provides a single parameter that may be used to characterize the collision process at ultracold temperatures. The variation of β/α with j is generally controlled by β except in special circumstances where the energy of the last bound state of the system approaches zero for a particular molecular excited state. Based on previous studies [13], β is expected to follow the exponential energy gap form,

$$\beta = P \exp(\Delta E_r/Q), \quad (4)$$

when only pure rotational transitions are included in the summation over inelastic channels. The energy gap ΔE_r is the difference in energy between the nearest allowable final rotational level and the initial rotational level j , and P and Q are fit parameters. For a linear rigid rotor, $\Delta E_r = -(4j - 2)B_e$ for homonuclear molecules and $\Delta E_r = -2jB_e$ for heteronuclear molecules, where B_e is the rotational constant. We take CO₂ as a symmetric linear rigid rotor, so that the former relation is applicable. Generally, if Q is comparable to B_e , then rotational relaxation decreases sufficiently rapidly with increasing j that rotationally excited molecules may be stable against collisional deexcitation.

Nonlinear molecules are more complicated. The rotational levels of an asymmetric top such as H₂O are labeled $j_{k_{-1},k_{+1}}$, where k_{-1} and k_{+1} are the projections of j on the body-fixed z' axis in the prolate and oblate limits. However, it is more convenient to label the rotational levels (j, τ) , where τ is a pseudo quantum number given by $\tau = k_{-1} - k_{+1}$. Even(odd) values of τ correspond to para-H₂O (ortho-H₂O). The ortho and para levels do not interconvert in nonreactive collisions

and can be treated separately. To fit β using Eq. (4), the energy gap is defined as the difference in energy between the nearest allowable final rotational level (j', τ) and the initial rotational level (j, τ) for a constant τ :

$$\Delta E_r = E(j' = j - 1, \tau) - E(j, \tau). \quad (5)$$

The rotational states of NH₃, a symmetric top, can be labeled $(jk\epsilon)$, where k is the projection of the rotational angular momentum on the body-fixed z' axis and ϵ is the parity index, which describes tunneling between the two equivalent umbrella configurations. For a given k , $j \geq k$, $k \geq 0$, and $\epsilon = \pm 1$, except for $k = 0$, where only $\epsilon = +1$ is allowed [21]. Rotational levels with $k = 3m$ are designated ortho-NH₃, while levels with $k = 3m \pm 1$ are para-NH₃, where $m = 0, 1, 2, \dots$. To fit β using Eq. (4), the energy gap is defined as the difference in energy between the nearest allowable final rotational level (j', k, ϵ) and the initial rotational level (j, k, ϵ) with the same quantum number k and parity,

$$\Delta E_r = E(j' = j - 1, k, \epsilon) - E(j, k, \epsilon). \quad (6)$$

The collisional stability of rotationally excited molecules also depends critically on the efficiency of rovibrational transitions. Generally, rovibrational transitions are less efficient than pure rotational transitions except in regions where vibration-rotation energy transfer is quasisonant. In such cases, the collision is characterized by very efficient transitions that follow a specific propensity rule. For linear molecules, the availability of a QRVR transition for a given initial state may be determined by examining the energy gap for the propensity rule. For example, the energy gap for the $\Delta j = -n\Delta v$ transition for a rotating harmonic oscillator is given by

$$\Delta E = \Delta E_v + \Delta E_r = w_e \Delta v + B_e n \Delta v (n \Delta v - 2j - 1), \quad (7)$$

where w_e is the vibrational frequency. Substitution of the n th-order quasisonant rotational level [13,16],

$$j_{\text{QR}}^{(n)} = \frac{w_e}{2nB_e} - \frac{1}{2}, \quad (8)$$

into Eq. (7) gives a positive energy gap of $B_e(n\Delta v)^2$ for both the upward and the downward vibrational transitions. Therefore, the relaxation efficiency for $j = j_{\text{QR}}^{(n)}$ will be dominated by pure rotational de-excitation for translational energies lower than $B_e n^2$. However, the $\Delta j = -n\Delta v$ energy gaps for $j \neq j_{\text{QR}}^{(n)}$ may be negative for nearby values of j . In the $j_{\text{QR}}^{(2)}$ case of homonuclear molecules, the nearest rotational levels with the same nuclear spin are $j = j_{\text{QR}}^{(2)} \pm 2$, which each have exothermic $\Delta j = -2\Delta v$ transitions that release $4B_e$ of energy. If the efficiency of pure rotational relaxation is low, then the $j = j_{\text{QR}}^{(2)} \pm 2$ levels will have total quenching rate coefficients that are significantly larger than those of the $j = j_{\text{QR}}^{(2)}$ level, and there will be sharp structures in the rotational distribution. Such structures are a unique feature of cold collisions. The small energy barriers that occur at $j = j_{\text{QR}}^{(n)}$ are easily overcome by translational energy at ordinary temperatures and rotational relaxation is generally very efficient. To produce highly rotationally excited

¹For plotting convenience, all figures display the magnitude of α .

TABLE I. Rotational constants, energy gap fit parameters, and quasis resonant rotational levels of linear molecules investigated in the present study. Spectroscopic constants are from Refs. [22] and [23]. All j_D and j_{QR} values are from harmonic approximation except $j_D = 31$ and 36 for H_2 and HD, respectively, which are exact.

| Molecule | ω_e (cm ⁻¹) | B_e (cm ⁻¹) | D_0 (cm ⁻¹) | j_D | $j_{QR}^{(2)}$ | $j_{QR}^{(4)}$ | P (Å) | Q (cm ⁻¹) | j_{max} |
|------------------------------|--------------------------------|---------------------------|---------------------------|-------|----------------|----------------|---------|-------------------------|-----------|
| H ₂ | 4401.2 | 60.85 | 36 118 | 31 | 18 | 9 | 0.2 | 200 | 18 |
| HD | 3813.1 | 45.66 | 36 406 | 36 | 20 | 10 | 0.5 | 137 | 26 |
| O ₂ | 1580.2 | 1.446 | 41 659 | 171 | 273 | 137 | 10.5 | 100 | 31 |
| CO | 2169.8 | 1.931 | 89 504 | 215 | 280 | 140 | 9.6 | 63 | 35 |
| CO ₂ ^a | $\nu_1 = 1388.17$ | 0.390 | 44 500 | 338 | 889 | 444 | 5 | 500 | 60 |
| CO ₂ ^b | $\nu_3 = 2349.16$ | | | | 1505 | 752 | | | |

^aSymmetric stretch, dissociation: $CO_2 \rightarrow O + C + O$ [23].

^bAsymmetric stretch, dissociation: $CO_2 \rightarrow O + CO$ [23].

molecules that are stable against collisional decay, it is usually necessary that the quasis resonant rotational level be less than the dissociation rotational level, which can be approximated by

$$j_D = \sqrt{\frac{D_e}{B_e}}, \quad (9)$$

where D_e is the equilibrium dissociation energy. Tables I and II give vibrational and rotational parameters for the linear and nonlinear molecules, respectively, included in the present study. The quasis resonant rotational quantum numbers listed in Tables I and II are obtained from the harmonic approximation using Eq. (8). For H₂O, $(B + C)/2$ was used to replace B_e , and for NH₃, B_e was replaced by B . The actual values depend on v and may be defined as the intersection points of the vibrationally upward and downward $\Delta j = -n\Delta v$ energy gaps using the exact molecular potential [13]. Tables I and II show that the second-order quasis resonant rotational levels for O₂, CO, CO₂, and NH₃ have values that are greater than the levels for dissociation. Therefore, the molecules do not possess bound levels that are collisionally stable and there would likely be efficient vibrational and rotational energy exchange for all excited states of these molecules. Although we do not consider vibrational motion in the present work, it is in the regions near $j_{QR}^{(n)}$ that interesting behavior will occur for linear molecules if the efficiency of pure rotational quenching is low. A similar situation may occur for nonlinear molecules (e.g.,

H₂O). Quasis resonant energy transfer is a general feature of molecular collisions [24] and it is expected that vibrational modes play an important role in the energy transfer process for ultracold collisions involving rotationally excited nonlinear molecules.

III. SCATTERING CALCULATIONS

Cross-section calculations were performed by applying the CC and CS methods. The interaction potentials adopted for all the scattering systems are listed in Ref. [25]. These potentials are considered to be superior to other potentials that are available for each system. All cross-section calculations were carried out using the nonreactive scattering code MOLSCAT [26]. Calculations were performed at a collision energy of 10^{-5} cm⁻¹, which was found to be sufficient for describing the collisions for each system in terms of the scattering length.² The calculations for CO₂, H₂O, and NH₃ assumed rigid molecular rotation. For H₂, HD, O₂, and CO molecules,

²At collision energies corresponding to buffer-gas cooling temperatures (~ 300 -mK) estimations of cross sections based on the scattering lengths, defined in the zero-temperature limit, may introduce some error, depending on the system. At energies corresponding to a few millikelvins, the estimated error is expected to be less than 10%, but it may be larger at higher energies.

TABLE II. Same as Table I but for nonlinear molecules H₂O and NH₃. Spectroscopic constants are from Ref. [23].

| Molecule | ν_2 (cm ⁻¹) | A (cm ⁻¹) | B (cm ⁻¹) | C (cm ⁻¹) | D_0 (cm ⁻¹) | j_D | $j_{QR}^{(2)}$ | P (Å) | Q (cm ⁻¹) | j_{max} |
|------------------|-----------------------------|-------------------------|-------------------------|-------------------------|---------------------------|-------|----------------|---------|-------------------------|-----------|
| H ₂ O | | | | | | | | | | |
| $\tau = 0$ | 1595 | 27.88 | 14.52 | 9.278 | 41 146 | 60 | 35 | 0.75 | 335 | 13 |
| $\tau = 2$ | | | | | | | | 0.64 | 350 | 13 |
| $\tau = -2$ | | | | | | | | 1.1 | 245 | 13 |
| $\tau = 1$ | | | | | | | | 0.66 | 365 | 13 |
| $\tau = -1$ | | | | | | | | 1.0 | 260 | 13 |
| NH ₃ | | | | | | | | | | |
| 0+ | 3337 | 9.9402 | 9.9402 | 6.3044 | 37 560 | 60 | 80 | 0.165 | 10 000 | 20 |
| 3+ | | | | | | | | 0.1 | 1440 | 20 |
| 1+ | | | | | | | | 0.3 | 390 | 15 |
| 2+ | | | | | | | | 0.346 | 265 | 15 |

the calculations allowed vibrational motion, however, ro-vibrational transitions have been excluded from the summation over inelastic channels in Eq. (1).

IV. RESULTS

In this work we calculated the real part, α , and imaginary part, β , of the scattering length of seven different systems with different potential energy surface properties in an effort to elucidate trends that can be explored in future cooling and trapping experiments. For each system, we also fitted β using the exponential energy gap form in Eq. (4). The fit parameters P and Q and the maximum values of rotational quantum number, j_{\max} , considered in this work are reported in Tables I and II.

The ratio β/α is a parameter that is not sensitive to fine details of the potential for a given system. It behaves like $p\alpha\sigma_j^{\text{in}}/\sigma_j^{\text{el}}$, where σ_j^{el} is the elastic scattering cross section from rotational state j , and σ_j^{in} is the total inelastic cross section including contributions from all possible de-excitation levels from state j . Figure 1 shows the ratio β/α for linear molecules (H_2 , HD, CO, O_2 , and CO_2) as a function of the initial rotational level for the first 10 excited levels of each system. Also shown in the figure is the same ratio for ortho- H_2O assuming a constant value for τ . The ratio for the nonlinear water molecule is shown to be comparable to that of the heavier linear systems. Generally, β/α decreases or remains constant with rotational excitation and increases with the reduced mass of the scattering system, except for CO. For H_2 and HD, β/α becomes small with increasing initial rotational excitation. This indicates that the inelastic cross section σ_j^{in} decreases rapidly with increasing initial rotational level j . The excited rotational states of H_2 and HD are therefore stable against collisional quenching when QRVR energy transfer is not allowed. This suggests that it would be possible to cool H_2 and HD without significant loss due to relaxation in a He bath. However, for CO, O_2 , and CO_2 ,

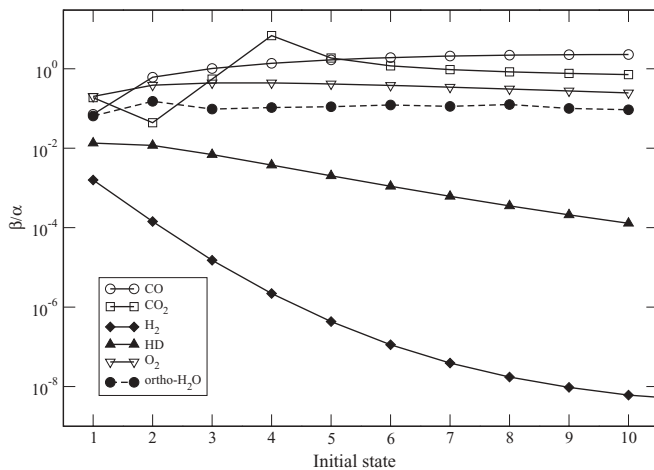


FIG. 1. Ratio of imaginary-to-real part of the complex scattering length as a function of the initial rotational level for CO (open circles), CO_2 (open squares), H_2 (filled diamonds), HD (filled triangles), O_2 (open triangles), and ortho- H_2O (filled circles) scattering with He.

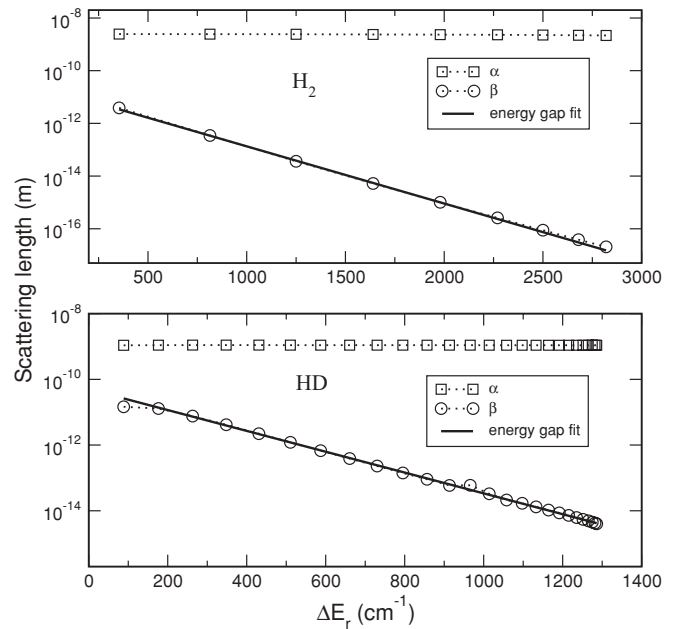


FIG. 2. Complex scattering lengths for He + H_2 (top) and He-HD (bottom) versus the energy gap.

the ratios are high, indicating that excited rotational levels of these molecules are susceptible to collisional quenching, in agreement with previous findings of Forrey [13] for He- O_2 . As the initial excitation level increases, the ratios approach constant values. The trend in Fig. 1 suggests that collisional quenching will be too efficient for the low rotational levels of CO, O_2 , and CO_2 to be viable candidates for cooling and trapping in the presence of He bath gas.

In Fig. 2 we present α , β , and energy gap fits for β using Eq. (4) for H_2 (top) and HD (bottom). Similar results are presented in Fig. 3 for O_2 and CO and in Fig. 4 for CO_2 .

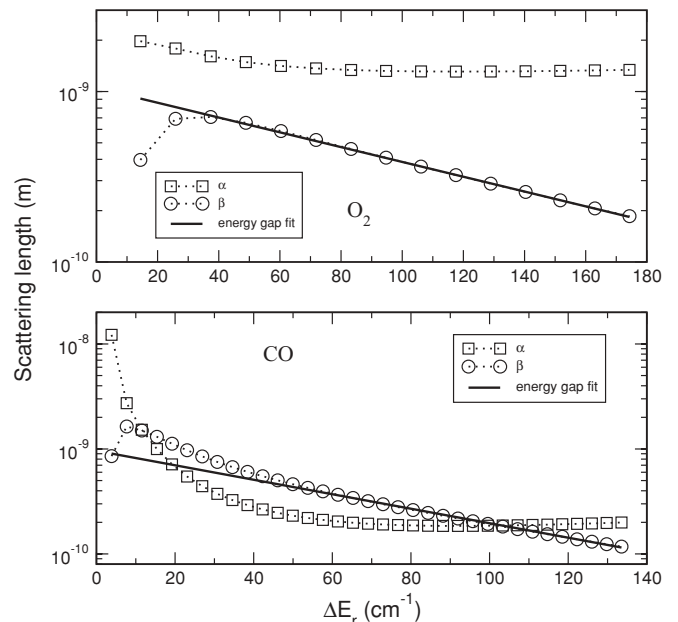


FIG. 3. Complex scattering lengths for He + O_2 (top) and He-CO (bottom) versus the energy gap.

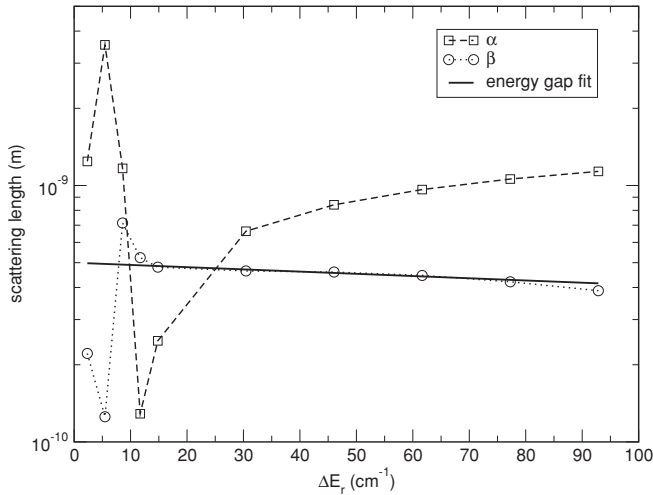


FIG. 4. Complex scattering lengths for He + CO₂ versus the energy gap.

Generally, the imaginary part of the scattering length for each scattering system decreases with increasing ΔE_r . For H₂, HD, and O₂, β is found to be much smaller than α , in agreement with previous calculations [13,27]. For He-CO, β shows a similar trend but α and β are comparable in magnitude for $j > 1$, in agreement with previous calculations of Balakrishnan *et al.* [28]. Although CO and O₂ have similar rotational constants, the rather pronounced difference in the variation of α with energy gap for these systems highlights the sensitivity of low-energy collisional data to details of the interaction potential. In addition, the finite dipole moment and additional de-excitation channels of CO (being heteronuclear) as well as the presence (or absence) of near-threshold atom-diatom bound or quasibound levels may also contribute to the differences.

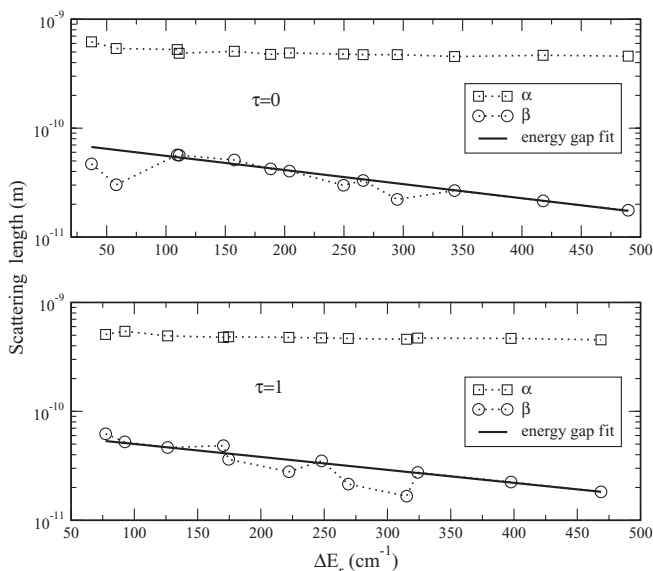


FIG. 5. Complex scattering lengths for He + H₂O versus the energy gap. Top: para-H₂O, $\tau = 0$. Bottom: ortho-H₂O, $\tau = 1$.

TABLE III. Cross sections for dominant transitions in para-H₂O in collisions with He at 10^{-5} cm⁻¹ for initial rotational levels $j = 1-13$ and $\tau = 0$. Numbers in parentheses indicate powers of 10.

| j | k_{-1} | k_{+1} | $\tau \rightarrow j'$ | k'_{-1} | k'_{+1} | τ' | Cross section (Å ²) |
|-----|----------|----------|-----------------------|-----------|-----------|---------|---------------------------------|
| 1 | 1 | 1 | 0 | 0 | 0 | 0 | 4.2395(3) |
| 2 | 1 | 1 | 0 | 2 | 0 | -2 | 2.6152(3) |
| 3 | 2 | 2 | 0 | 2 | 1 | 0 | 2.1796(3) |
| 4 | 2 | 2 | 0 | 4 | 1 | 3 | 3.4905(3) |
| 5 | 3 | 3 | 0 | 5 | 2 | 4 | 2.2297(3) |
| 6 | 3 | 3 | 0 | 6 | 2 | 4 | 3.2839(3) |
| 7 | 4 | 4 | 0 | 7 | 3 | 5 | 1.9509(3) |
| 8 | 4 | 4 | 0 | 8 | 3 | 5 | 2.5975(3) |
| 9 | 5 | 5 | 0 | 9 | 4 | 6 | 1.6221(3) |
| 10 | 5 | 5 | 0 | 10 | 4 | 6 | 1.8701(3) |
| 11 | 6 | 6 | 0 | 11 | 5 | 7 | 1.2159(3) |
| 12 | 6 | 6 | 0 | 12 | 5 | 7 | 1.3424(3) |
| 13 | 7 | 7 | 0 | 13 | 6 | 8 | 9.4980(2) |

Scattering lengths for He-CO₂, which include rotational levels $j = 2-60$ are shown in Fig. 4. In this case, for low ΔE_r , both α and β show an oscillatory structure. For high ΔE_r , β is smaller than α .

We also performed scattering length calculations for the nonlinear molecules H₂O and NH₃. The magnitudes of α , as well as β , are similar for the two nonlinear molecules. Figure 5 shows the scattering lengths of para-H₂O with $\tau = 0$ and ortho-H₂O with $\tau = 1$ as functions of ΔE_r , along with the energy gap fits for β . For both cases, β generally decreases with increasing ΔE_r and is significantly smaller than α . The dominant quenching transitions and corresponding cross sections at a collision energy of 10^{-5} cm⁻¹ from initial H₂O states with $\tau = 0$ (para-H₂O) and $\tau = 1$ (ortho-H₂O), for rotational quantum number j up to 13 are shown in Tables III and IV, respectively. In cold collisions, the quenching cross sections are dominated by transitions with $\Delta j = j' - j = 0$ and $\Delta \tau = \tau' - \tau = -2$ for both para- and ortho-H₂O, except for the initial states $(j, \tau) = (1, 0)$ and $(3, 0)$, for which quenching transitions are dominated by $\Delta j = -1$ and $\Delta \tau = 0$.

TABLE IV. Same as Table III but for ortho-H₂O with initial states corresponding to $\tau = 1$.

| j | k_{-1} | k_{+1} | $\tau \rightarrow j'$ | k'_{-1} | k'_{+1} | τ' | Cross section (Å ²) |
|-----|----------|----------|-----------------------|-----------|-----------|---------|---------------------------------|
| 1 | 1 | 0 | 1 | 1 | 0 | -1 | 3.6019(3) |
| 2 | 2 | 1 | 1 | 2 | 1 | -1 | 2.6590(3) |
| 3 | 2 | 1 | 1 | 3 | 1 | -1 | 3.4186(3) |
| 4 | 3 | 2 | 1 | 4 | 2 | -1 | 2.5995(3) |
| 5 | 3 | 2 | 1 | 5 | 2 | -1 | 2.8992(3) |
| 6 | 4 | 3 | 1 | 6 | 3 | -1 | 2.1682(3) |
| 7 | 4 | 3 | 1 | 7 | 3 | -1 | 2.2720(3) |
| 8 | 5 | 4 | 1 | 8 | 4 | -1 | 1.6884(3) |
| 9 | 5 | 4 | 1 | 9 | 4 | -1 | 1.6962(3) |
| 10 | 6 | 5 | 1 | 10 | 5 | -1 | 1.2767(3) |
| 11 | 6 | 5 | 1 | 11 | 5 | -1 | 1.2648(3) |
| 12 | 7 | 6 | 1 | 12 | 6 | -1 | 9.8519(2) |
| 13 | 7 | 6 | 1 | 13 | 6 | -1 | 9.5595(2) |

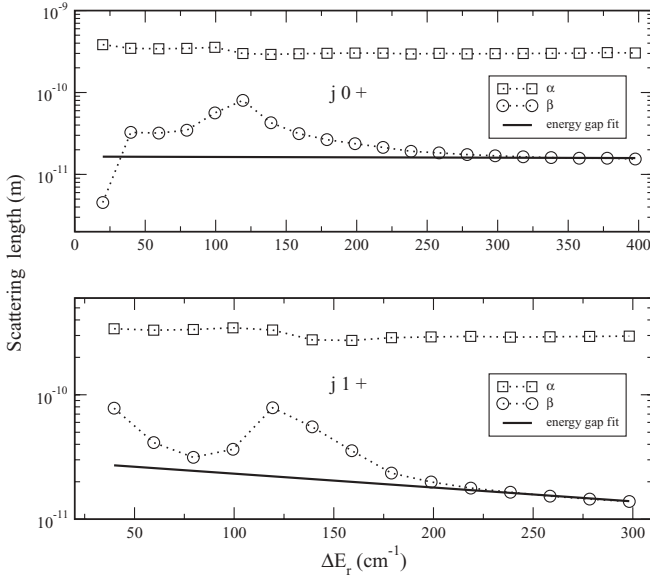


FIG. 6. Complex scattering lengths for He + NH₃ versus the energy gap. Top: ortho-NH₃, $k = 0$, $\epsilon = +$. Bottom: para-NH₃, $k = 1$, $\epsilon = +$.

The same trend ($\Delta j = 0$ and $\Delta \tau = -2$) persists for j beyond 13 and for initial states with $\tau = 2, -2$, and -1 . It should be emphasized that in Fig. 5, α and β are shown versus ΔE_r corresponding to $\Delta j = -1$ and $\Delta \tau = 0$, which are not the dominant transitions. However, β is obtained from the total quenching cross section, which includes contributions from all possible de-excitation channels. This demonstrates that the exponential energy gap fit for β is reasonable when using ΔE_r defined by Eq. (5).

Figure 6 shows the variation of scattering lengths with energy gap for He-NH₃. The energy gap ΔE_r corresponds to transitions with $\Delta j = -1$, $\Delta k = 0$, and the same parity. Results are presented for ortho-NH₃ with $k = 0$, $\epsilon = +$ and para-NH₃ with $k = 1$, $\epsilon = +$. It is shown that for both ortho- and para-NH₃, β is significantly smaller than α . However, for ortho-NH₃, β approaches a constant value with increasing ΔE_r , while for para-NH₃, it decreases with increasing ΔE_r . The dominant quenching transitions and corresponding cross sections from selected initial states with $k = 0$ and $\epsilon = +$

TABLE V. Cross sections for dominant transitions in ortho-NH₃ in collisions with He at 10^{-5} cm⁻¹ for rotational levels $j = 2-10$, $k = 0$, and $\epsilon = +$. Numbers in parentheses indicate powers of 10.

| j | k | $\epsilon \rightarrow j'$ | k' | ϵ' | Cross section (\AA^2) |
|-----|-----|---------------------------|------|-------------|----------------------------------|
| 2 | 0 | + 0 | 0 | + | 2.0771(3) |
| 3 | 0 | + 3 | 3 | + | 9.4377(3) |
| 4 | 0 | + 4 | 3 | + | 1.7048(3) |
| 5 | 0 | + 5 | 3 | + | 3.7984(3) |
| 6 | 0 | + 6 | 3 | + | 3.6956(3) |
| 7 | 0 | + 7 | 3 | + | 1.4182(3) |
| 8 | 0 | + 8 | 3 | + | 1.1314(3) |
| 9 | 0 | + 9 | 3 | + | 1.1128(3) |
| 10 | 0 | + 10 | 3 | + | 1.1369(3) |

TABLE VI. Same as Table V but for para-NH₃ with $k = 1$ and $\epsilon = +$ initial states.

| j | k | $\epsilon \rightarrow j'$ | k' | ϵ' | Cross section (\AA^2) |
|-----|-----|---------------------------|------|-------------|----------------------------------|
| 2 | 1 | + 1 | 1 | - | 5.5916(3) |
| 3 | 1 | + 2 | 1 | - | 1.3929(3) |
| 4 | 1 | + 4 | 2 | + | 6.6462(2) |
| 5 | 1 | + 5 | 2 | + | 1.1549(3) |
| 6 | 1 | + 6 | 4 | + | 2.2504(3) |
| 7 | 1 | + 7 | 4 | + | 1.2292(3) |
| 8 | 1 | + 7 | 1 | + | 8.9600(2) |
| 9 | 1 | + 9 | 4 | + | 5.7079(2) |
| 10 | 1 | + 10 | 4 | + | 5.7818(2) |

(ortho-NH₃) and $k = 1$ and $\epsilon = +$ (para-NH₃) for j up to 10 are presented in Tables V and VI, respectively. Generally, the quenching cross sections are dominated by parity-preserving $\Delta j = 0$ and $\Delta k = 3$ transitions. The same trend persists for j beyond 10 and also for initial states with $k = 3$, $\epsilon = \pm$; $k = 1$, $\epsilon = -$; and $k = 2$, $\epsilon = \pm$. Meyer [29] investigated the rotational excitation of NH₃ in collisions with He at a collision energy of 140 meV in a counterpropagating beam experiment and found a propensity for collisions with $\Delta k = \pm 3$ for para-NH₃ and with $\Delta k = 3$ for ortho-NH₃. Our results are generally in agreement with this finding, though the experiment was performed at a much higher energy.

Tables V and VI indicate that these trends are not satisfied for the lowest j since the final states for $\Delta k = 3$ transitions are absent for initial states 20+, 21+, and 31+. Some additional anomalies occur in the case of para-NH₃, where the dominant transitions 41+ \rightarrow 42+ and 51+ \rightarrow 52+ correspond to minimization in energy transfer, as opposed to the $\Delta k = 3$ propensity. Further, we note that typically the transitions with the next-largest cross sections have magnitudes comparable to those of the dominant transitions listed in Tables V and VI. This fact and the anomalies already discussed, are primarily responsible for the unusual behavior of β at $\Delta E_r \lesssim 120$ cm⁻¹ shown in Fig. 6. For higher j (higher ΔE_r), the exponential energy gap form of Eq. (4) gives a reasonable fit for β when defined by Eq. (6) for both ortho- and para-NH₃.

V. CONCLUSION

We have investigated ultracold collisions of linear molecules (H₂, HD, CO, O₂, and CO₂) and nonlinear molecules (H₂O and NH₃) with helium atoms. It has been found that the ratio of the imaginary to real components of the scattering length, β/α , generally increases with decreasing rotational constant. As the energy gap ΔE_r for rotational transitions increases, β becomes significantly smaller than α , except for CO. The imaginary part β can be fitted to the exponential energy gap form for both linear and nonlinear molecules. Rotational quenching of H₂O is dominated by $\Delta j = 0$ and $\Delta \tau = -2$ transitions, while that of NH₃ is dominated by $\Delta j = 0$ and $\Delta k = 3$ transitions. In both cases, the dominant transitions preserve parity. Emission spectra would provide signatures [14] of the predicted structure in the

rotational distribution of β . Among the systems investigated here, the best candidate for producing rotationally excited states that are collisionally stable in the presence of a cold He bath gas appears to be H_2 and, to a lesser extent, HD, for which β/α is very small. However, an interesting QRVR structure in the rotational distribution of β was predicted for highly excited CO [15], and it appears that highly rotationally excited water molecules may show a similar QRVR effect if an extrapolation of the exponential energy gap fits to high j is valid. We believe that the illustrative results presented here will benefit future

experimental studies of these or similar systems as methods to cool and trap neutral molecules become more robust and widespread.

ACKNOWLEDGMENTS

B.H.Y. and P.C.S. acknowledge support from NASA Grant No. NNX07AP12G. R.C.F. acknowledges support from NSF Grant No. PHY-0854838, and N.B. acknowledges support from NSF Grant No. PHY-0855470.

-
- [1] J. Doyle, B. Friedrich, R. V. Krems, and F. Masnou-Seeuws, *Eur. Phys. J. D* **31**, 149 (2004).
- [2] R. V. Krems, *Int. Rev. Phys. Chem.* **24**, 99 (2005).
- [3] G. Quemener, N. Balakrishnan, and A. Dalgarno, in *Cold Molecules: Theory, Experiment, and Applications*, edited by R. V. Krems, W. C. Stwalley, and B. Friderich (CRC Press, Boca Raton, FL, 2009), pp. 69–124.
- [4] E. Bodo and F. A. Gianturco, *Int. Rev. Phys. Chem.* **25**, 313 (2006).
- [5] N. Balakrishnan, B. C. Hubartt, L. Ohlinger, and R. C. Forrey, *Phys. Rev. A* **80**, 012704 (2009).
- [6] J. M. Doyle, B. Friedrich, J. Kim, and D. Patterson, *Phys. Rev. A* **52**, R2515 (1995).
- [7] J. D. Weinstein, R. deCarvalho, T. Guillet, B. Friedrich, and J. M. Doyle, *Nature (London)* **395**, 148 (1998).
- [8] D. M. Villeneuve, S. A. Aseyev, P. Dietrich, M. Spanner, M. Y. Ivanov, and P. B. Corkum, *Phys. Rev. Lett.* **85**, 542 (2000).
- [9] J. Li, J. T. Bahns, and W. C. Stwalley, *J. Chem. Phys.* **112**, 6255 (2000).
- [10] R. C. Forrey, N. Balakrishnan, A. Dalgarno, M. R. Haggerty, and E. J. Heller, *Phys. Rev. Lett.* **82**, 2657 (1999).
- [11] A. J. McCaffery, *J. Chem. Phys.* **113**, 10947 (2000).
- [12] R. C. Forrey, *Phys. Rev. A* **63**, 051403 (2001).
- [13] R. C. Forrey, *Phys. Rev. A* **66**, 023411 (2002).
- [14] R. C. Forrey, *Eur. Phys. J. D* **31**, 409 (2004).
- [15] P. M. Florian, M. Hoster, and R. C. Forrey, *Phys. Rev. A* **70**, 032709 (2004).
- [16] A. Mack, T. K. Clark, R. C. Forrey, N. Balakrishnan, T.-G. Lee, and P. C. Stancil, *Phys. Rev. A* **74**, 052718 (2006).
- [17] B. H. Yang, H. Perera, N. Balakrishnan, R. C. Forrey, and P. C. Stancil, *J. Phys. B* **39**, S1229 (2006).
- [18] P. Barletta, J. Tennyson, and P. F. Barker, *Phys. Rev. A* **78**, 052707 (2008).
- [19] M. Y. Choi, G. E. Douberly, T. M. Falconer, W. K. Lewis, C. M. Lindsay, J. M. Merritt, P. L. Stiles, and R. E. Miller, *Int. Rev. Phys. Chem.* **25**, 15 (2006).
- [20] N. Balakrishnan, V. Kharchenko, R. C. Forrey, and A. Dalgarno, *Chem. Phys. Lett.* **280**, 5 (1997).
- [21] S. Green, *J. Chem. Phys.* **64**, 3463 (1978).
- [22] K. P. Huber and G. Herzberg, *Molecular Spectra and Molecular Structure, Vol. IV. Constants of Diatomic Molecules* (Van Nostrand Reinhold, New York, 1979).
- [23] G. Herzberg, *Molecular Spectra and Molecular Structure, Vol. III. Electronic Spectra of Polyatomic Molecules* (Van Nostrand Reinhold, New York, 1966).
- [24] A. Ruiz and E. J. Heller, *Mol. Phys.* **104**, 127 (2006).
- [25] He- H_2 , HD: P. Muchnick and A. Russek, *J. Chem. Phys.* **100**, 4336 (1994); He-CO: T. G. A. Heijmen, R. Moszynski, P. E. S. Wormer, and A. van der Avoird, *ibid.* **107**, 9921 (1997); He- O_2 : G. C. Groenenboom and I. M. Struniewicz, *ibid.* **113**, 9562 (2000); He- CO_2 : H. Ran and D. Q. Xie, *ibid.* **128**, 124323 (2008); He- H_2O : K. Patkowski, T. Korona, R. Moszynski, B. Jeziorski, and K. Szalewicz, *J. Mol. Struct. (Theochem.)* **591**, 231 (2002); He- NH_3 : M. P. Hodges and R. J. Wheatley, *J. Chem. Phys.* **114**, 8836 (2001).
- [26] J. M. Hutson and S. Green, MOLSCAT computer code version 14. Collaborative Computational Project 6 (Engineering and Physical Sciences Research Council UK, London, 1994).
- [27] J. L. Nolte, B. H. Yang, P. C. Stancil, T.-G. Lee, N. Balakrishnan, R. C. Forrey, and A. Dalgarno, *Phys. Rev. A* **81**, 014701 (2010).
- [28] N. Balakrishnan, A. Dalgarno, and R. C. Forrey, *J. Chem. Phys.* **113**, 621 (2000).
- [29] H. Meyer, *J. Phys. Chem.* **99**, 1101 (1995).